Supplementary Information

Unveiling the Complex Configurational Landscape of the Intralayer Cavities in a Crystalline Carbon Nitride

Magnus Pauly, Julia Kröger, Viola Duppel, Corban Murphey, James Cahoon, Bettina Lotsch and Paul A. Maggard

Flux Synthesis of Poly(Triazine Imide) (PTI/LiCl):

The preparation of PTI/LiCl is begins with weighing 17.6 mmol potassium chloride and 7.9 mmol melamine and transferring these into a mortar and pestle and grinding until the mixture appears to be a homogenous white powder. To this mixture 22 mmol of lithium chloride was added and ground together. This powder was then loaded into a reaction vessel that was approximately 10 inches long and a radius of 0.5 inches and sealed under vacuum. The reaction vessel was placed vertically into a muffle furnace and heated at a rate of 10 ^{o}C/min until 470 ^{o}C is reached. This temperature was held for 36 hrs, after which the furnace was cooled at a rate of 2 ^{o}C/hr until the temperature reaches 350 ^{o}C. The furnace was then shut off and allowed to radiatively cool to room temperature. The heating rate, reaction time, and cooling rate were all optimized over course of numerous repeated experiments. The product is repeatedly washed with de-ionized water to dissolve the excess salt and isolate the crystalline PTI/LiCl powder, which had a white to lightly beige color.

Flux-Exchange Synthesis of PTI/CuCl:

An anhydrous CuCl/KCl mixture (60/40 molar ratio) was combined with the PTI/LiCl powder within an argon-filled glovebox. For this reaction, 0.2mmol of PTI/LiCl and CuCl/KCl was loaded at a quantity of up to 0.86 mmol of Cu. The reactants were ground together until the mixture appeared to be a homogenous powder. The reactants were transferred into a fused-silica tube that was sealed under vacuum. This reaction vessel was heated at a rate of ~10 ^{o}C/min until the furnace reached 450 ^{o}C. This temperature was held for 24 h after which the furnace is cooled at a rate of 2 ^{o}C/min until the temperature reached 300 ^{o}C. At this point, the furnace was shut off and allowed to radiatively cool to room temperature. The resulting product was isolated from the salt flux by washing, as described for PTI (above).

Table S1. Elemental analysis (ICP-MS) of PTI/LiCl and PTI/CuCl loaded with increasing Cu(I) cation in the flux exchange reaction.

PTI/Cu$_x$Cl	**Li**	**C**	**N**	**Cu**	**H**	**Cl**
Loaded as x = 0.15	1.921	5.992	9.080	0.154	3.394	1.057
Calculated from formula	1.85	6	9	0.15	1.85	1
Loaded as x = 0.35	1.617	6.002	9.102	0.369	3.577	1.115
Calculated from formula	1.65	6	9	0.35	1.65	1
Loaded as x = 1.8*	0.179	5.999	8.931	1.064	3.794	0.950
Calculated from formula	0.2	6	9	1.8	0.2	1

PTI/LiCl	**Li**	**C**	**N**	**N/A**	**H**	**Cl**
Experimental	2.009	6.003	9.161	0	3.752	1.155
Calculated from formula	2	6	9	0	2	1

* At the loading of x = 1.8, a change in the crystal structure is observed and is currently under investigation.

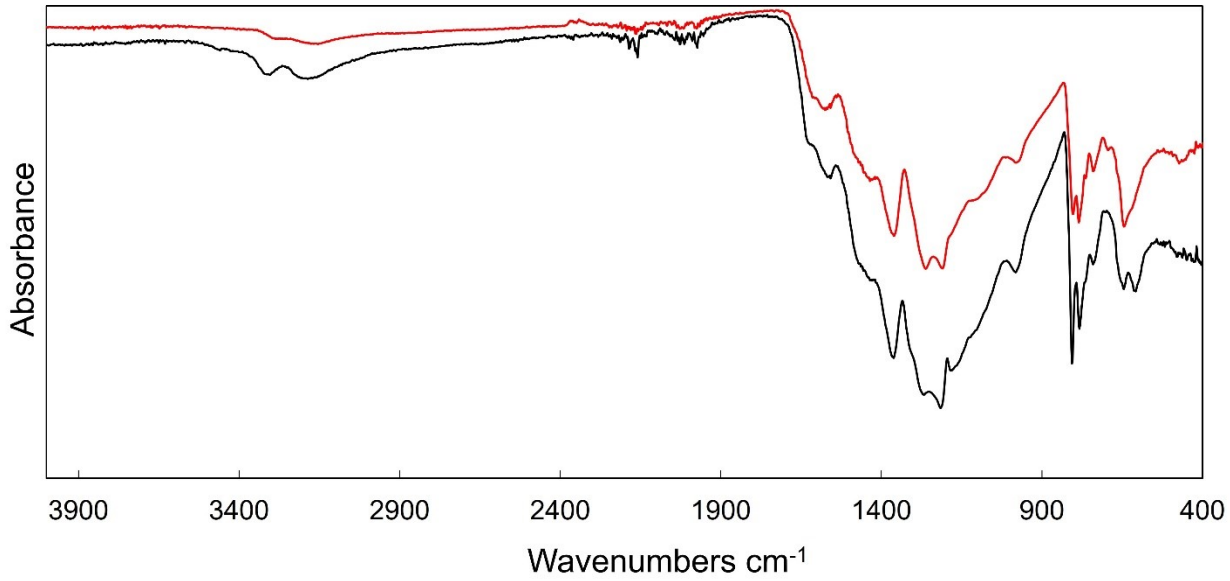

Figure S1. FTIR data of PTI/LiCl (black line) and PTI/CuCl (red line) powders.

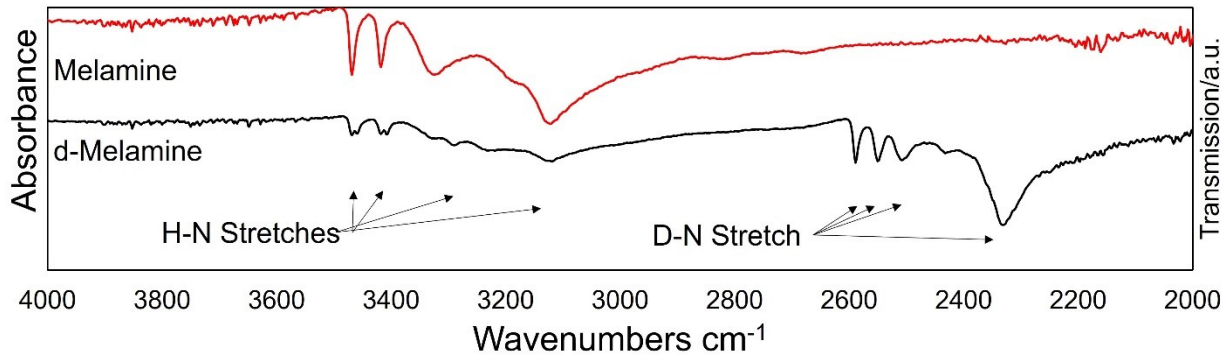

Figure S2. FTIR data of the deuterated (black line) and non-deuterated (red line) melamine precursor.

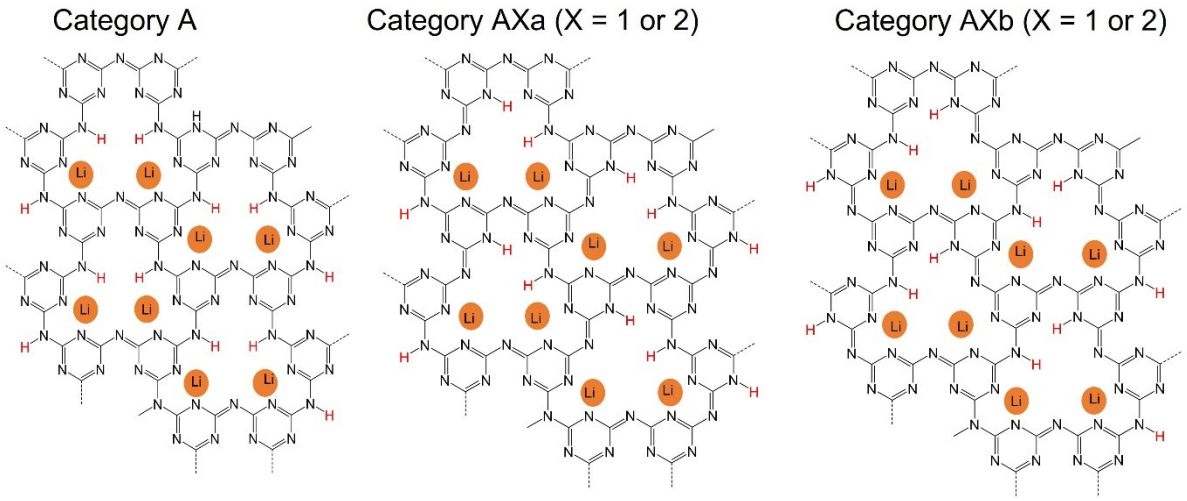

Figure S3. Structural drawings of the three H-atom environments (100% N-triazine (left), and 50% N-triazine and 50% N-imide (middle, left) for the category A substructure of Li cations.

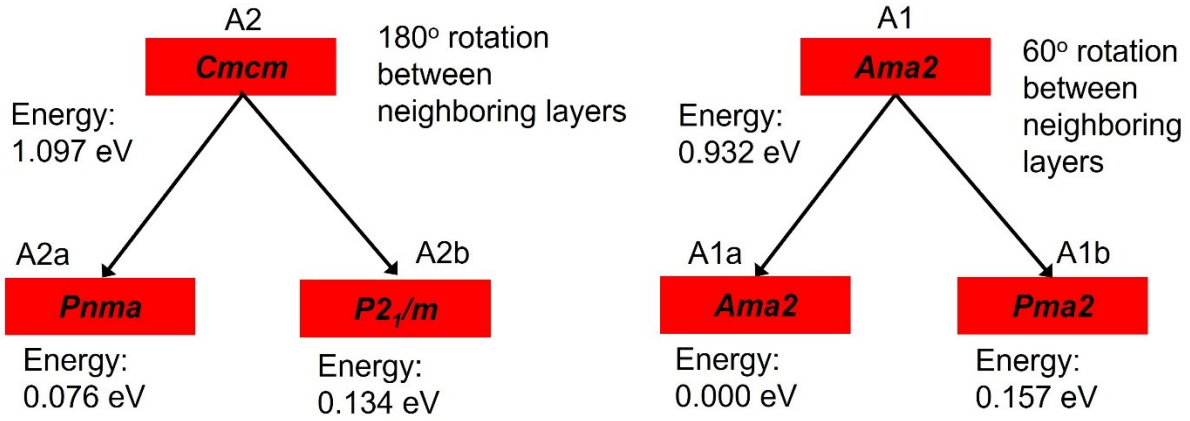

Figure S4. A tree diagram illustrating the relationships between the models with and 60° or 180° layer-to-layer stacking (upper) and shifting of the H atoms (lower) to N-triazine groups, as shown in Figure S3 for the Category A model. All energies are relative to the A1a structural model.

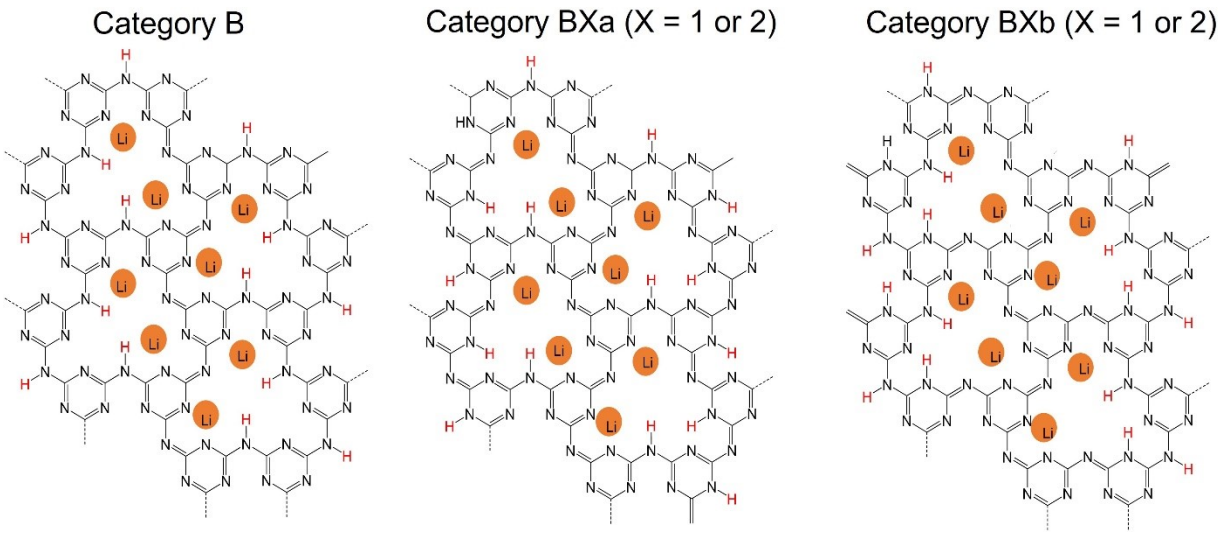

Figure S5. Structural drawings of the three H-atom environments (100% N-triazine (left), and 50% N-triazine and 50% N-imide (middle, left) for the category B substructure of Li cations.

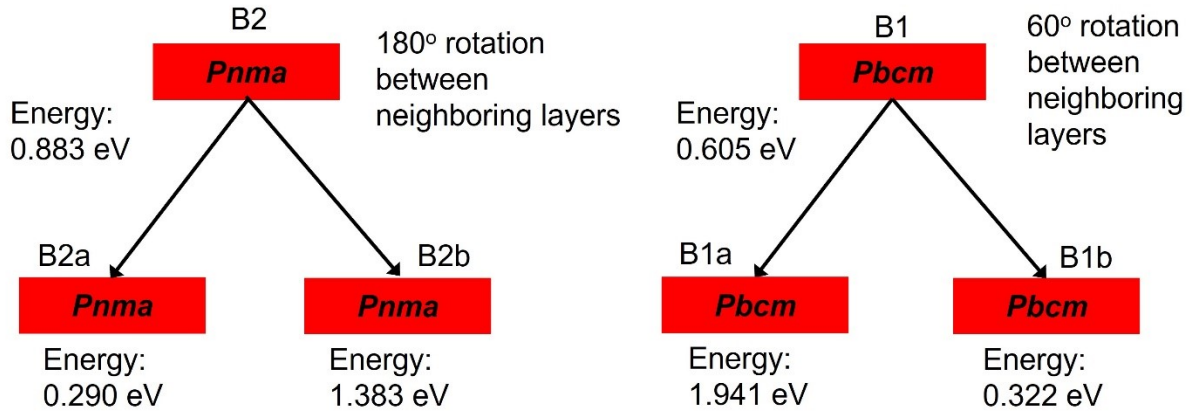

Figure S6. A tree diagram illustrating the relationships between the models with and 60° or 180° layer-to-layer stacking (upper) and shifting of the H atoms (lower) to N-triazine groups, as shown in Figure S5 for the Category B model. All energies are relative to the A1a structural model.

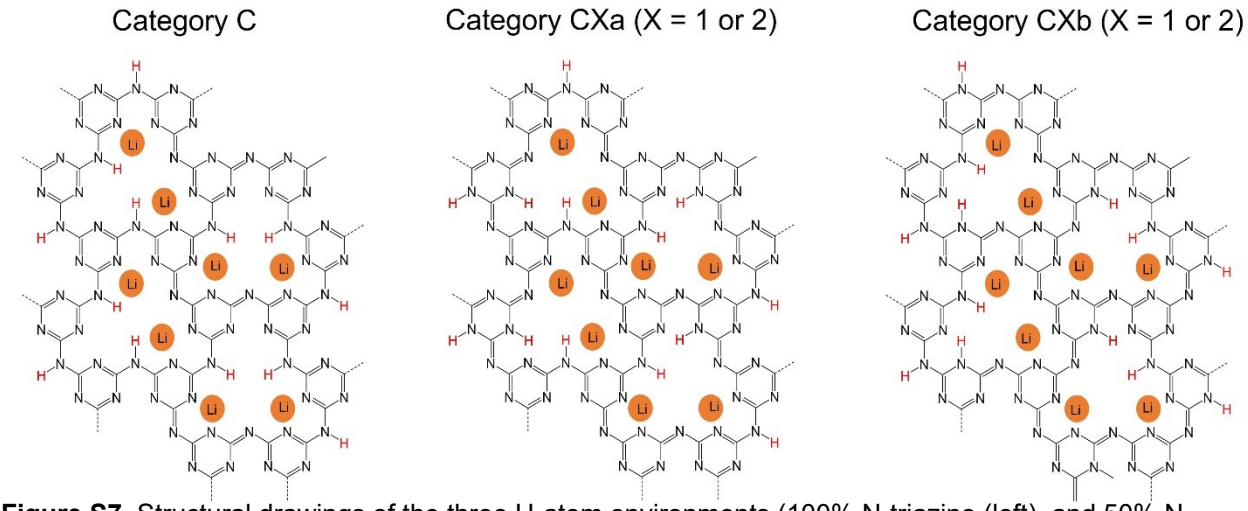

Figure S7. Structural drawings of the three H-atom environments (100% N-triazine (left), and 50% N-triazine and 50% N-imide (middle, left) for the category C substructure of Li cations.

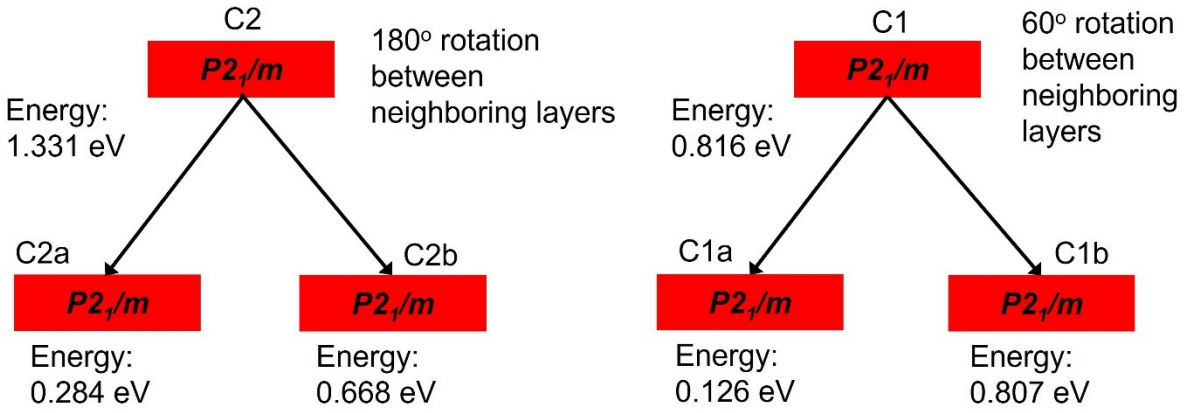

Figure S8. A tree diagram illustrating the relationships between the models with and 60° or 180° layer-to-layer stacking (upper) and shifting of the H atoms (lower) to N-triazine groups, as shown in Figure S7 for the Category C model. All energies are relative to the A1a structural model.

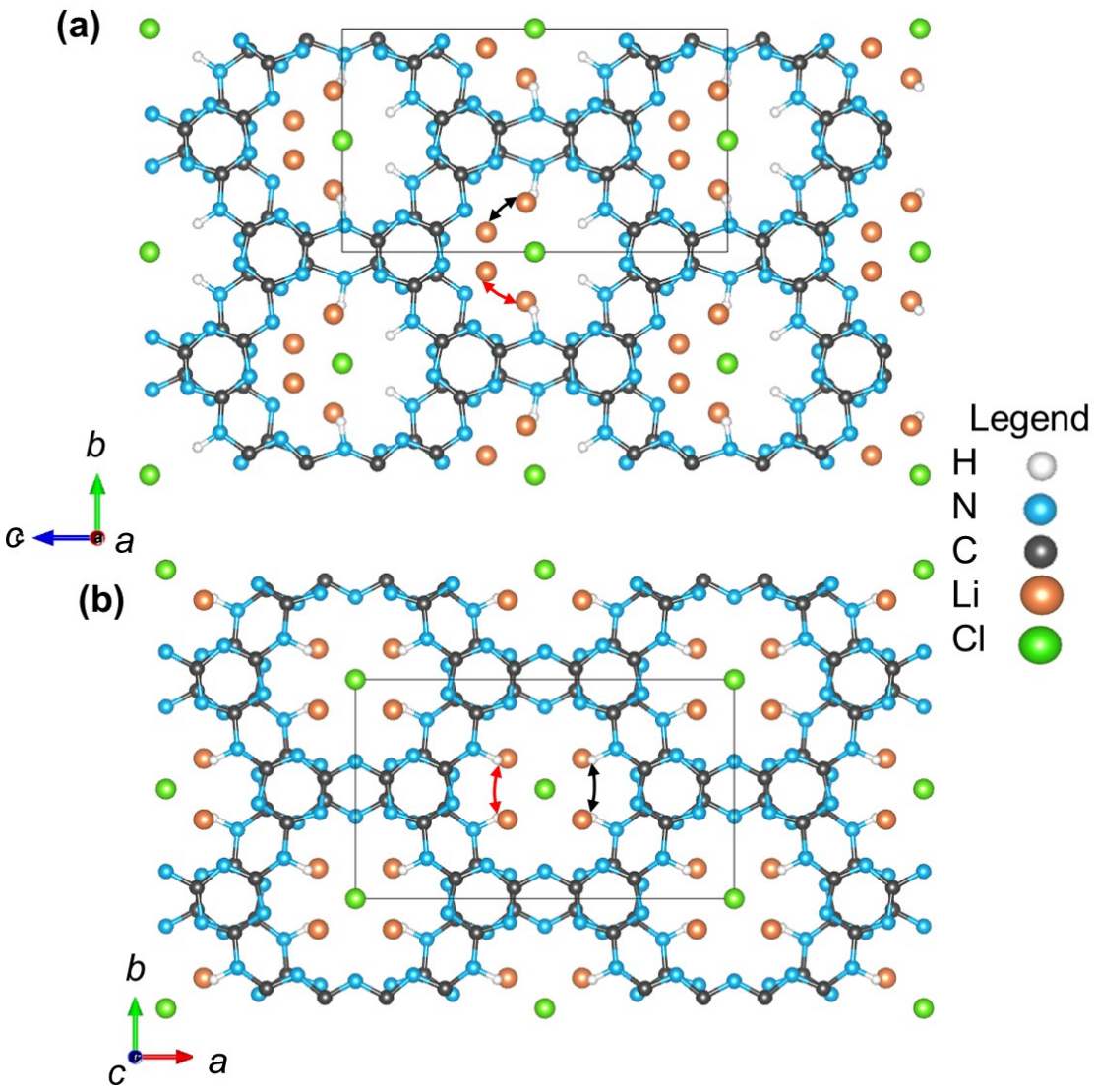

Figure S9. Structural models which illustrate the difference in the layer-to-layer rotation of Li cations in either a 60^{o} orientation (upper; A1) or a 180^{o} orientation (lower; A2). All H atoms in these models are coordinated to the N-imide bridges.

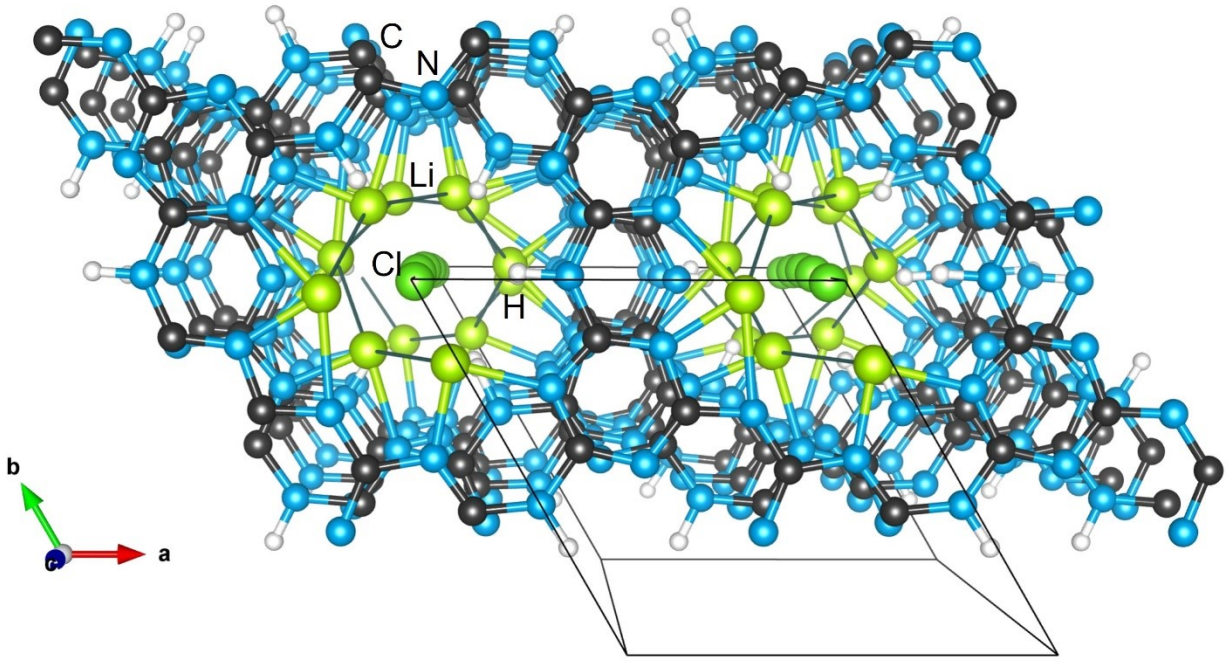

Figure S10. Structural model which illustrates an example of a helical conformation in the layer-to-layer arrangement of the Li/H atoms, with a tripled *a*-axis for the A1 model in Table 1. All H atoms in this model are coordinated to the N-imide bridges.

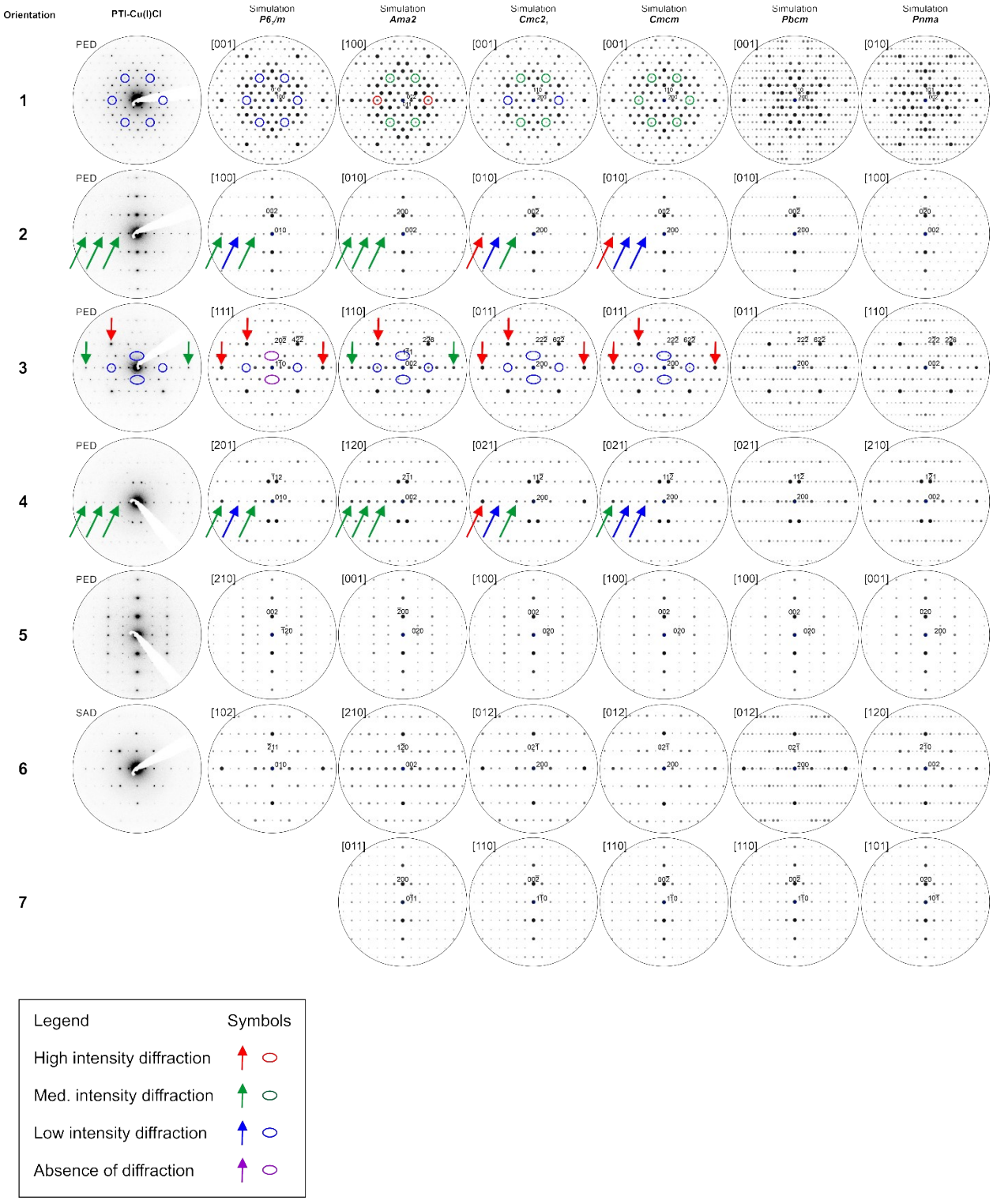

Figure S11. A comparison of electron diffraction data versus simulated patterns for PTI/CuCl, with colored arrows/rings to indicate similarities and differences.

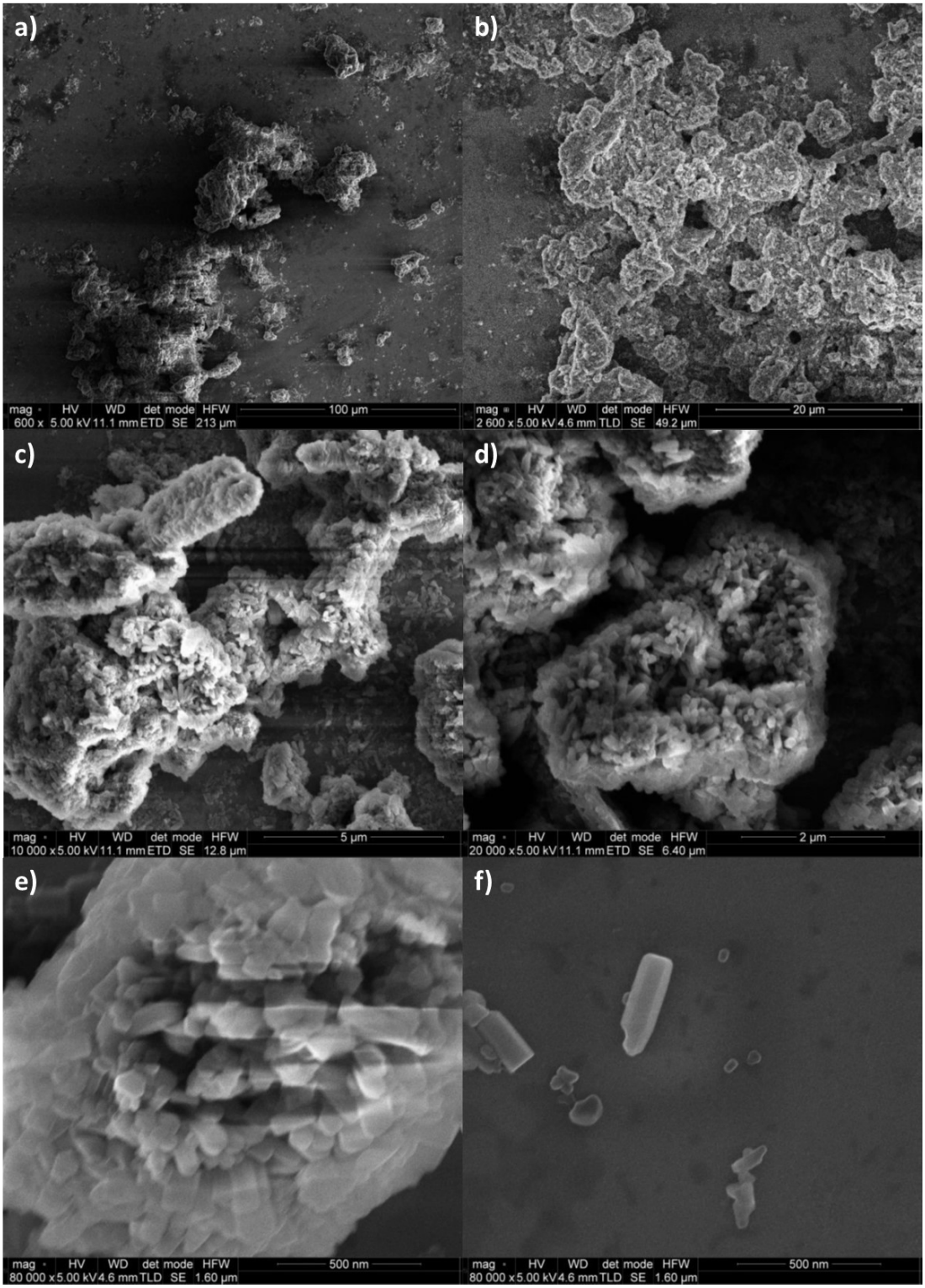

Figure S12. SEM images of PTI/LiCl crystallites at different magnifications: a) 100 µm, b) 20 µm, c) 5 µm, d) 2 µm, e) 500 nm, and f) a single flake at 500 nm. Samples were prepared by sonicating in a methanol/water solution and drop casting onto standard glass microscopy slides (Fisher Scientific) coated with ~3 nm of ITO by sputtering (Kurt Lesker PVD 75) to facilitate imaging, and images were acquired with an FEI Helios 600 Nanolab Dual Beam System.

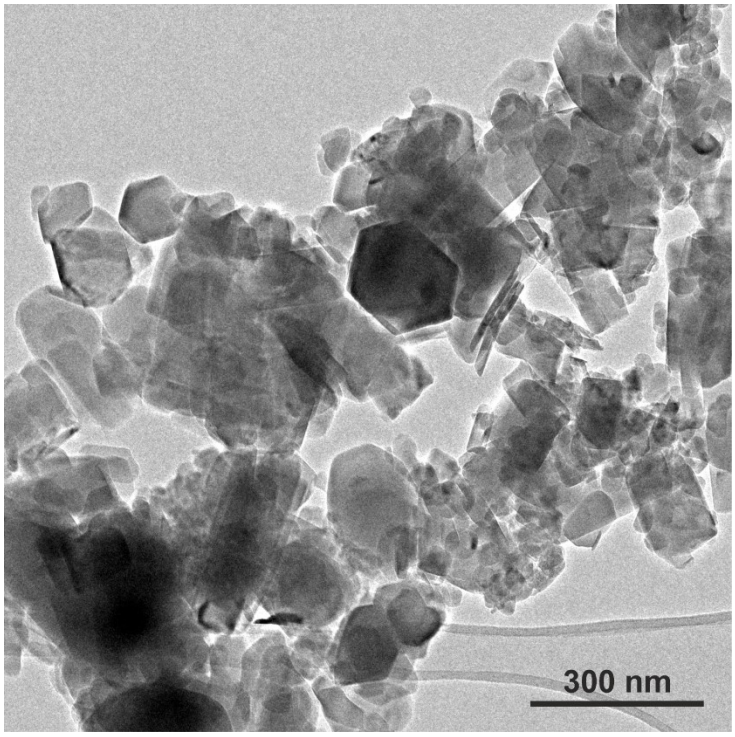

Figure S13. Wide area zoom of the TEM images of PTI/CuCl, showing the various crystallite orientations and morphologies. Powder ground in a mortar and distributed onto a holey carbon/Ni grid was studied with a Philips CM 30 ST microscope (300 kV, LaB6 cathode) equipped with a spinning star device enabling the use of precession electron diffraction (PED). Simulations of the diffraction patterns were obtained with the JEMS software package.

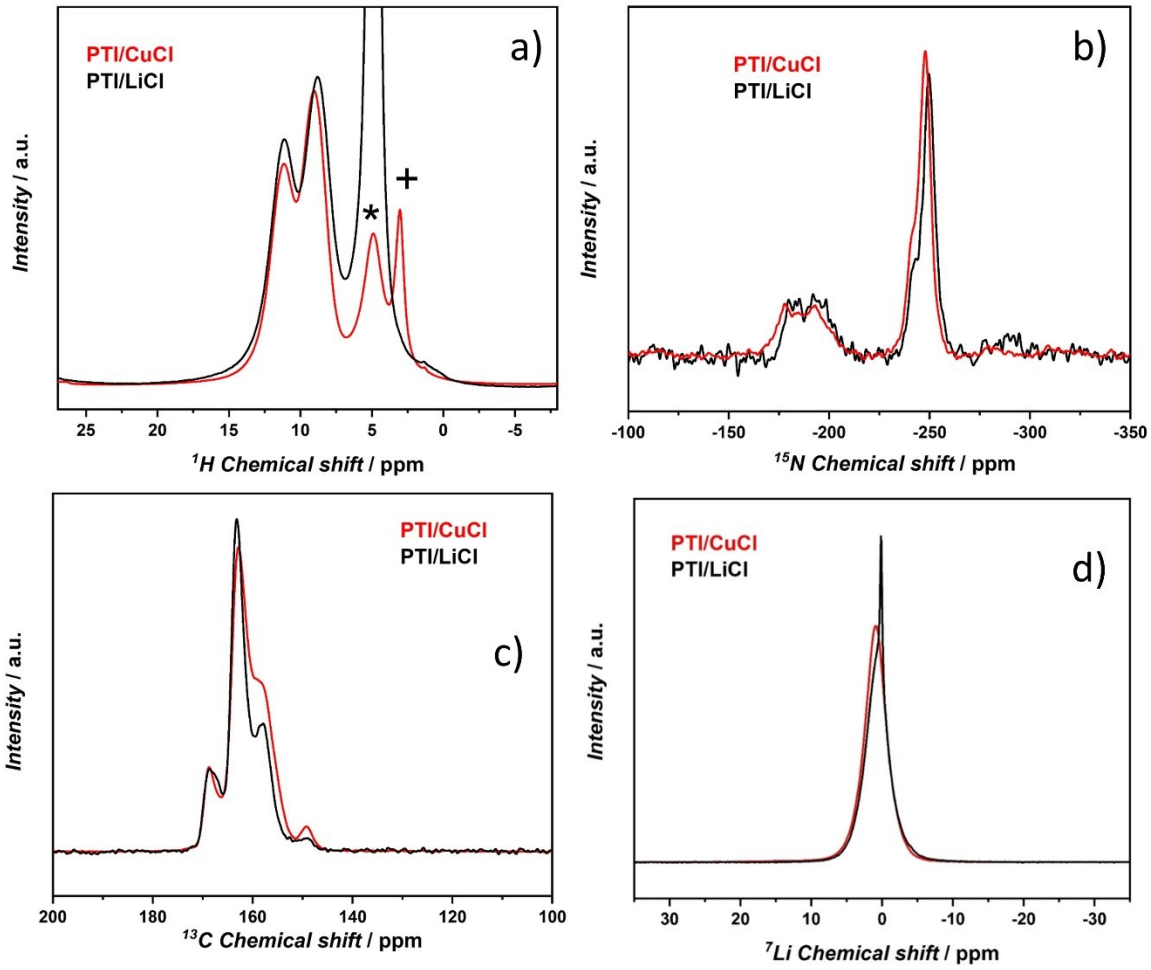

Figure S14. Plots of the solid-state NMR data of PTI/LiCl and PTI/CuCl for their ^{1}H spectrum (a), ^{15}N spectrum (b), ^{13}C spectrum (c) and the ^{7}Li spectrum (d). The (*) and (+) peaks label signals arising from water in both PTI/MCl (M = Li and Cu) and contamination from washing the PTI/CuCl product in a basic hydroxide solution, respectively.

```
data_A1a_Ama2_d-PTI
_pd_phase_name  A1a
_cell_length_a  6.7321(4)
_cell_length_b  8.4597(21)
_cell_length_c  14.614(4)
_cell_angle_alpha  90
_cell_angle_beta   90
_cell_angle_gamma  90
_cell_volume  832.29(11)
_exptl_crystal_density_diffrn  2.0030
_symmetry_cell_setting  orthorhombic
_symmetry_space_group_name_H-M  "A m a 2"
loop_
   _space_group_symop_id
   _space_group_symop_operation_xyz
    1  x,y,z
    2  1/2-x,y,z
    3  1/2+x,-y,z
    4  -x,-y,z
    5  x,1/2+y,1/2+z
    6  1/2-x,1/2+y,1/2+z
    7  1/2+x,1/2-y,1/2+z
    8  -x,1/2-y,1/2+z

loop_
  _atom_site_label
  _atom_site_type_symbol
  _atom_site_fract_x
  _atom_site_fract_y
  _atom_site_fract_z
  _atom_site_occupancy
```

```
  _atom_site_adp_type
  _atom_site_U_iso_or_equiv
  _atom_site_site_symmetry_multiplicity
C1    C   0.75000   0.59585   0.75823   1.000   Uiso 0.018     4
C5    C   0.75000   0.34061   0.81378   1.000   Uiso 0.0181210 4
C9    C   0.75000   0.55399   0.91386   1.000   Uiso 0.0181210 4
C13   C   0.25000   0.40303   0.23462   1.000   Uiso 0.0181210 4
C17   C   0.25000   0.65623   0.17571   1.000   Uiso 0.0181210 4
C21   C   0.25000   0.44929   0.07523   1.000   Uiso 0.0181210 4
N1    N   0.75000   0.66108   0.84253   1.000   Uiso 0.022     4
N5    N   0.75000   0.43927   0.74248   1.000   Uiso 0.0215063 4
N9    N   0.75000   0.40004   0.90183   1.000   Uiso 0.0215063 4
N13   N   0.25000   0.34706   0.14994   1.000   Uiso 0.0215063 4
N17   N   0.25000   0.56278   0.25000   1.000   Uiso 0.0215063 4
N21   N   0.25000   0.60523   0.08766   1.000   Uiso 0.0215063 4
N25   N   0.75000   0.68498   0.68186   1.000   Uiso 0.0215063 4
N29   N   0.25000   0.81595   0.81092   1.000   Uiso 0.0215063 4
N33   N   0.25000   0.37160   0.99315   1.000   Uiso 0.0215063 4
Li1   Li  0.75000   0.86008   0.89921   1.000   Uiso 0.013     4
Li5   Li  0.75000   0.23022   0.97202   1.000   Uiso 0.0125000 4
Cl1   Cl  0.50000   0.00000   1.00490   1.000   Uiso 0.044     4
H1    H   0.75000   0.76928   0.13946   0.250   Uiso 0.012     4
H5    H   0.75000   0.61790   0.62363   0.250   Uiso 0.0124000 4
D1    D   0.75000   0.76928   0.13946   0.750   Uiso 0.0124000 4
D5    D   0.75000   0.61790   0.62363   0.750   Uiso 0.0124000 4

_cell_formula_units_Z  4
_chemical_formula_sum  "C6 H2 Cl Li2 N9"
_chemical_formula_weight  250.99
_pd_proc_ls_profile_function
;
Von Dreele-Jorgenson-Windsor function parameters
```

```
   alpha, beta-0, beta-1, beta-q, sig-0, sig-1, sig-2, sig-q, X, Y:
    0.122, 0.011, -0.006, 0.059, 18.775, -274.704, 394.379, 61.748, 3.298, 18.443,
  Crystallite size in microns with "isotropic" model:
  parameters: Size, G/L mix
    4.000, 1.000,
  Microstrain, "isotropic" model (10^6^ * delta Q/Q)
    parameters: Mustrain, G/L mix
    4523.011, 1.000,
;
_pd_proc_ls_prof_R_factor     0.07656
_pd_proc_ls_prof_wR_factor    0.07500
_gsas_proc_ls_prof_R_B_factor   0.09720
_gsas_proc_ls_prof_wR_B_factor  0.12773
_pd_proc_ls_prof_wR_expected  0.00575
_diffrn_radiation_probe  neutron
_pd_meas_2theta_fixed  90.000
_pd_proc_ls_background_function
;
Background function: "chebyschev-1" function with 30 terms:
    84.798, -6.076, 5.713, -1.142, 2.154, -1.605, 0.246, 1.035,
    -0.209, -0.779, -0.487, 1.411, -0.339, -1.075, 1.764, -1.243,
    0.498, 0.054, -0.454, 0.240, 0.628, -0.869, 0.543, 0.002,
    -0.117, 0.213, -0.326, 0.578, -0.322, 0.346,
;
_diffrn_ambient_temperature  300
_diffrn_ambient_pressure  100
```

```
data_Cmc21_PTI_CuCl
_pd_phase_name  "Cmc21 PTI/CuCl"
_cell_length_a  14.727(5)
_cell_length_b  8.5152(31)
_cell_length_c  6.7343(4)
_cell_angle_alpha  90
_cell_angle_beta   90
_cell_angle_gamma  90
_cell_volume  844.48(11)
_exptl_crystal_density_diffrn  2.302
_symmetry_cell_setting  orthorhombic
_symmetry_space_group_name_H-M  "C m c 21"
loop_
   _space_group_symop_id
   _space_group_symop_operation_xyz
    1  x,y,z
    2  -x,y,z
    3  x,-y,1/2+z
    4  -x,-y,1/2+z
    5  1/2+x,1/2+y,z
    6  1/2-x,1/2+y,z
    7  1/2+x,1/2-y,1/2+z
    8  1/2-x,1/2-y,1/2+z

loop_
  _atom_site_label
  _atom_site_type_symbol
  _atom_site_fract_x
  _atom_site_fract_y
  _atom_site_fract_z
  _atom_site_occupancy
```

```
  _atom_site_adp_type
  _atom_site_U_iso_or_equiv
  _atom_site_symmetry_multiplicity
N1    N   0.08451   0.39380   0.18380   1.000   Uiso 0.010   8
N2    N   0.75665   0.05923   0.66272   1.000   Uiso 0.010   8
N3    N   0.15386   0.66314   0.17380   1.000   Uiso 0.010   8
N4    N   0.00000   0.63632   0.20190   1.000   Uiso 0.010   4
N5    N   0.18288   0.80413   0.67870   1.000   Uiso 0.010   8
C1    C   0.17787   0.36184   0.19770   1.000   Uiso 0.010   8
C2    C   0.73998   0.89712   0.67770   1.000   Uiso 0.010   8
C3    C   0.08324   0.55420   0.18190   1.000   Uiso 0.010   8
Li1   Li  0.89050   0.11580   0.69530   0.440   Uiso 0.010   8
Li2   Li  0.50000   0.25430   0.67100   0.440   Uiso 0.010   4
H1    H   0.00000   0.75430   0.20300   0.330   Uiso 0.010   4
H2    H   0.13170   0.85810   0.67100   0.330   Uiso 0.010   8
Cl    Cl  0.00000   0.98352   0.93593   1.000   Uiso 0.010   4
H4    H   0.50000   0.25430   0.67100   0.330   Uiso 0.010   4
H3    H   0.89050   0.11580   0.69530   0.330   Uiso 0.010   8
Cu1   Cu  0.89061   0.11664   0.66505   0.186(5)  Uiso 0.010   8
Cu2   Cu  0.50000   0.28075   0.62697   0.309(11)  Uiso 0.010   4

loop_  _atom_type_symbol _atom_type_number_in_cell
 C   24
 H   7.92
 Cl  4
 Cu  2.721
 Li  5.280
 N   36

_cell_formula_units_Z  4
_chemical_formula_sum  "C6 H1.98 Cl Cu0.68 Li1.32 N9"
_pd_proc_ls_profile_function
```

;

Finger-Cox-Jephcoat function parameters U, V, W, X, Y, SH/L:

peak variance(Gauss) = Utan(Th)^2^+Vtan(Th)+W:

peak HW(Lorentz) = X/cos(Th)+Ytan(Th); SH/L = S/L+H/L

U, V, W in (centideg)^2^, X & Y in centideg

39.127, -2.985, 2.198, 0.035, 3.516, 0.070,

Crystallite size in microns with "isotropic" model:

parameters: Size, G/L mix

10.000, 1.000,

Microstrain, "isotropic" model (10^6^ * delta Q/Q)

parameters: Mustrain, G/L mix

9919.587, 1.000,

;

_diffrn_radiation_type K\a~1,2~

loop_

_diffrn_radiation_wavelength

_diffrn_radiation_wavelength_wt

_diffrn_radiation_wavelength_id

0.70926 1.0 1

0.71354 0.0000 2

_refine_ls_R_F_factor 0.11729

_refine_ls_R_Fsqd_factor 0.13830

_pd_proc_ls_prof_R_factor 0.04484

_pd_proc_ls_prof_wR_factor 0.06016

_gsas_proc_ls_prof_R_B_factor 0.06553

_gsas_proc_ls_prof_wR_B_factor 0.09988

_pd_proc_ls_prof_wR_expected 0.02998

_diffrn_radiation_probe x-ray

_diffrn_radiation_polarisn_ratio 0.7000

_pd_proc_ls_background_function

;

Background function: "chebyschev" function with 15 terms:

729.746, -582.740, -82.173, -5426.464, 12610.813, 55533.430,

-105723.561, -222112.078, 390266.580, 392985.212, -670524.708,

-320313.235, 538481.467, 99029.926, -164506.193,

;

_diffrn_ambient_temperature 300

_diffrn_ambient_pressure 100

#--eof--#